Tumescent antibiotic injections for drug-resistant infections.

John P. Koulakis[a,*], Joshua Rouch[b], Nhan Huynh[b], Holden Wu[c], James Dunn[d], Seth Putterman[a]

[a]*Department of Physics and Astronomy, University of California Los Angeles, Los Angeles, California 90095, USA*
[b]*Department of Surgery, Division of Pediatric Surgery, University of California Los Angeles, Los Angeles, California 90095, USA*
[c]*Department of Radiology, University of California Los Angeles, Los Angeles, California 90095, USA*
[d]*Department of Surgery. Division of Pediatric Surgery, Stanford Children's Health, 300 Pasteur Drive, Alway M116, Stanford, California 94305, USA*

Abstract

Tumescent injections are a method of delivering concentrated antibiotic directly to skin infections. We present a detailed physical picture, based on diffusion-weighted magnetic resonance imaging, computed tomography, and 3D-scanning on live and dead pigs, that highlights its potential to effectively treat drug-resistant wound infections. Subcutaneous tissue has the remarkable ability to expand several times in thickness upon injections of high volumes of fluid. Pores are opened up, dispersing the fluid and dramatically increasing tissue permeability. The tumescent fluid (here, physiological saline) remains localized for a couple hours on its own, or over 7 hr with 1:100 000 dilute epinephrine. Adding high concentrations of antibiotic to the tumescent fluid will expose invading organisms - even drug-resistant ones - to levels above their minimum inhibitory concentration for many hours, yet the total dose will remain low. Clinical trials testing this technique should begin immediately.

Keywords: Tumescent tissue, antibiotic-resistant infections, 3D scanning, chronic wounds

Can skin infections and chronic wounds (diabetic ulcers, pressure sores, etc.) be treated with targeted antibiotic injections? If you infuse concentrated antibiotic into the tissue directly underneath an infected wound, will it cure the infection? The chief advantage of local treatments is that drugs can be delivered directly to the affected regions at higher concentration with reduced risk of systemic toxicity. Topical application can be effective in some cases, but not for treating chronic, especially antibiotic-resistant, wounds. What about infusing antibiotic into the volume of the infection itself in a way that causes it to completely permeate the tissue?

This question appears simple to answer. Surely *someone* must have tried targeted antibiotic injections in the nearly hundred years since humanity discovered penicillin. Yet there is a surprising void in the literature on this topic. Perhaps someone tried

*Corresponding Author: John Koulakis, Email: koulakis@physics.ucla.edu.

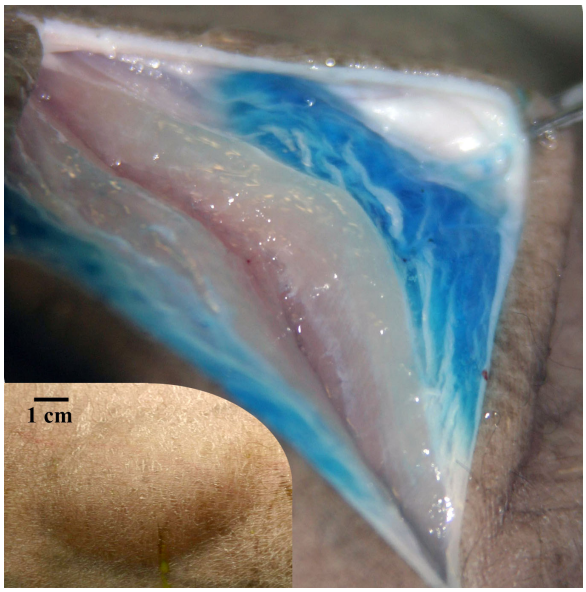

Figure 1: A tumescent injection of 10 mL saline (dyed blue) causes a large, conspicuous bleb to form in the skin of a dead pig (inset). Slicing into it reveals that the liquid is trapped in the subcutaneous tissue, which was forced to expand to accommodate the liquid.

but it was not effective and not reported. Or perhaps no one has tried because there are good medical reasons and/or rationalizations why it could not work, or, in fact, be dangerous. For instance, a concentrated antibiotic may be toxic to tissue and cause necrosis. Further, injecting fluid into an infection is a great way to make it spread (Duran-Reynals, 1929, 1942); but is this still the case if the fluid is an antibiotic? Even if the injection is safe in itself, if it is absorbed and distributed to the entire body rapidly, then the net effect of the injection is equivalent to a systemic dose, and the benefits of a local treatment are lost.

For antibiotic injections to be effective, they must be done in such a way where: 1) The drug is at least tolerated by skin and subcutaneous tissue at concentrations high enough to kill the offending organism. 2) The drug thoroughly permeates the entire volume where the organism resides, including micro-pores in the interstitial matrix. A simple injection may be coarsely distributed in a root-like, or river-delta like, pattern, leaving regions in-between rivulets untreated; this is to be avoided. 3) The drug must reside in the infected tissue long enough to kill the infection. There is a trade-off between criteria 1) and 3); higher concentrations will require less time to eradicate the infection.

We argue that tumescent antibiotic injections can fulfill all these criteria and will become a safe, effective, and irreplaceable method of curing skin and soft-tissue infections, particularly chronic wounds, and especially antibiotic-resistant ones. Criterion 1) is easily satisfied. For instance, Nicolau and Silberg (2015) report that cefazolin at a concentration of 1.024 mg mL^{-1} is above the minimum inhibitory concentration (MIC) of all but 1 of 1239 MRSA isolates tested. Although the cefazolin concentration that would cause necrosis in subcutaneous tissue is not known, Harb et al. (2009) tested ceftriaxone at 350× higher concentration with no sign of toxicity. Further, slow, subcutaneous antibiotic infusions are regularly performed as an alternative to oral or IV delivery (Azevedo et al., 2012), without adverse effect. Herein we present evidence aggregated from various experiments on live and dead pigs, including computed tomography (CT), diffusion-weighted magnetic resonance imaging (DW-MRI), and 3D scanning, that demonstrates that tumescent injections can also achieve criteria 2) and 3).

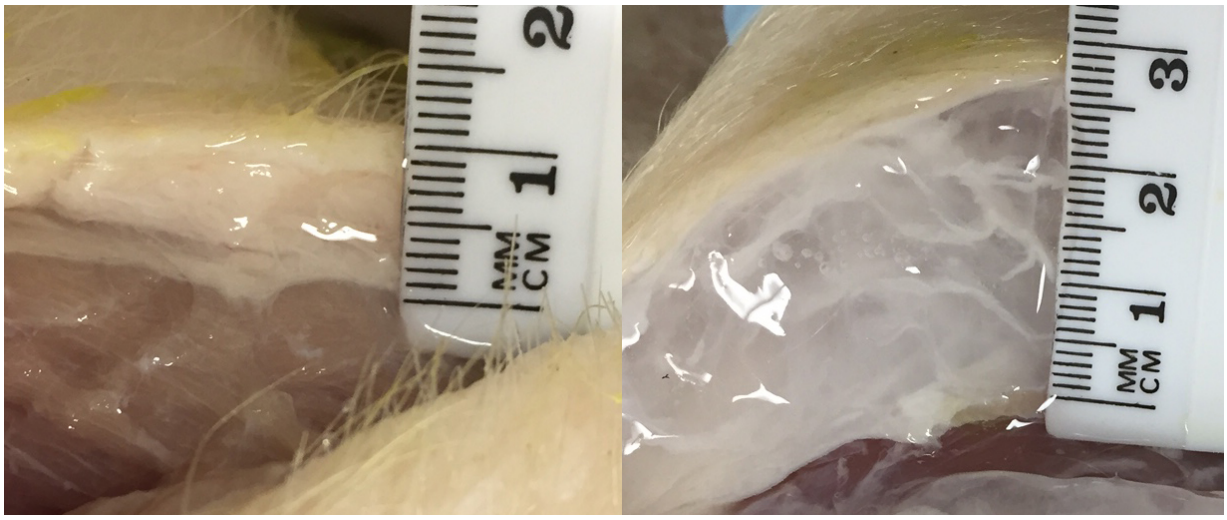

Figure 2: Subcutaneous tissue of a Yorkshire pig can swell 4-5× in thickness upon injection of saline.

Tumescent injections thoroughly disperse antibiotic

Tumescent injections are performed by inserting a needle or cannula into subcutaneous tissue and infusing sufficient volumes of fluid at a fast enough rate to cause swelling. This is distinguished from hypodermoclysis (HDC) or subcutaneous administration of antibiotics, where care is taken to avoid swelling. HDC is becoming a popular method of hydrating geriatric patients due to its simplicity and safety, where liters of fluids, usually saline, are infused at a rate of about 1-2.5 mL min^{-1} for many hours. Similar infusion rates are used when administering antibiotics subcutaneously (but not tumescently) as an alternative to the intravenous (IV) route. As the non-tumescent subcutaneous route is used as an alternative for *systemic* delivery, research on it has focused on the altered pharmacokinetics (Harb et al., 2009; Azevedo et al., 2012; Frasca et al., 2010), not on its potential for *localized* treatment. These infusion rates, which are small compared to the body's circulation, are chosen so that the additional fluid is dispersed before it can build up and cause swelling. Tumescent infusions are done 10-100× faster, with total volumes ranging between 0.1-2 L, depending on the surface area to be covered. A 10 mL tumescent injection of blue-dyed saline into a dead Yucatán mini-pig leaves a bleb about 4 cm across, and 1 cm thick (figure 1). Amazingly, the fluid gets trapped within the extracellular matrix, and forces it to expand to several times its initial volume. Figure 2 shows an expansion of about 4× in the subcutaneous tissue of a dead Yorkshire pig, transforming it from opaque and fleshy in appearance, to semi-transparent and glass-like.

Even more remarkable, is that despite the trauma of expansion, the tissue recovers and heals quickly, on its own. The tumescent technique was invented by Jeffrey Klein in the late 1980s as an alternative method of liposuction (Klein, 1987), that has since proven itself a safe, low-complications procedure and become common practice (Hanke et al., 2004). Under this procedure, up to several liter of saline

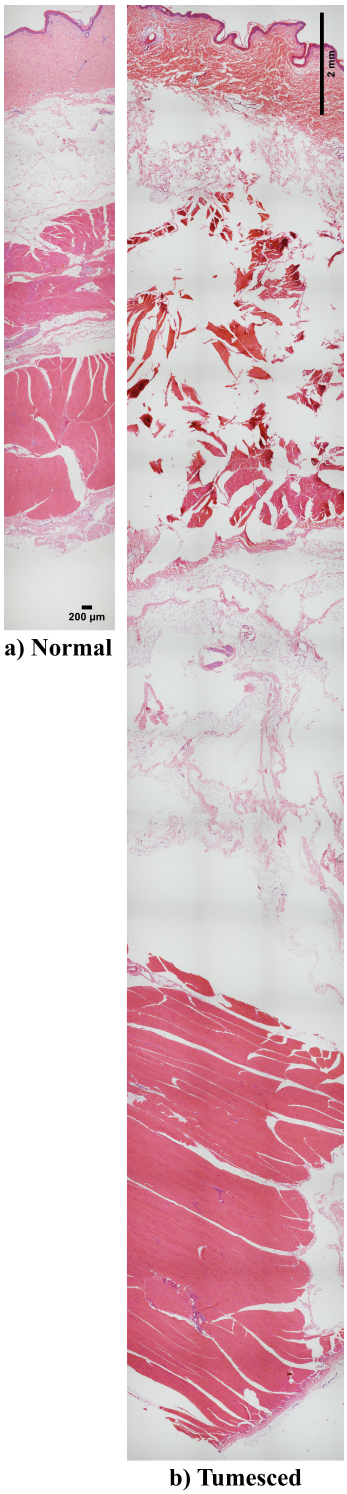

Figure 3: Histology of a) normal and b) tumescent subcutaneous tissue after a 5 mL saline injection.

are infused into subcutaneous tissue before a suction cannula is inserted and fat is removed. Patients recover in a few days, faster and with less bruising, than without the tumescent technique (Klein, 1990). Trauma to, and recovery of, tumesced tissue was never an issue in 688 patients followed for six months (Hanke et al., 2004).

The hydraulic conductivity (Darcy permeability) of normal subcutaneous tissue is low, about 10^{-11} cm^4 dyne^{-1} sec^{-1} (Swabb et al., 1974), but can increase by over four orders of magnitude upon swelling (Guyton et al., 1966). As the tumescence expands, the length scale of the extracellular matrix grows as well, opening up pores, and filling the extra volume with the infusate. Not surprisingly, the forced expansion mechanically fractures subcutaneous tissue on a microscopic level, as revealed by histological samples of normal and tumesced tissue (figure 3), increasing permeability further. Low tissue permeability prevents infections from spreading by keeping them isolated. Indeed, Duran-Reynals (1929, 1942) demonstrated that increasing tissue permeability near an infection causes it to spread perilously, and so it is generally advised to avoid injecting fluids into an infection.

We acknowledge the risk involved, but note that if the fluid is a concentrated antibiotic, it is substantially mitigated. In fact, considering the fractured nature of the tumesced tissue, we see an opportunity to treat infections by using an antibiotic solution as the tumescent fluid. In this light, the enhanced permeability works in our favor. The injection drives concentrated solution throughout the infected volume by forcing pores that might harbor bacteria to open, and flushing them with antibiotic. If small, unexpanded pockets remain, they are still surrounded by the solution, and the antibi-

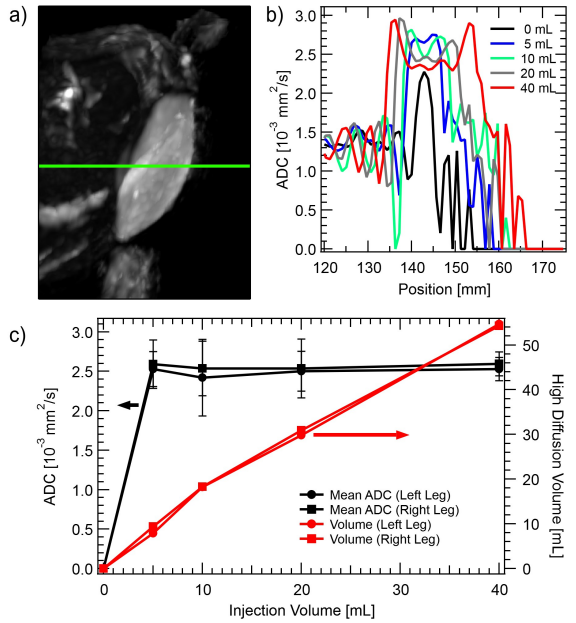

Figure 4: Diffusion MRI imaging easily detects tumescent tissue due to its high permeability. Panel a) is an axial image of the left thigh and pelvis of a juvenile Yucatán pig viwed from the legs up after 40 mL have been infused into the thigh. Lighter regions correspond to higher ADC. Lineouts along the green line in a) are shown in b), as more liquid is infused into the subcutaneous tissue. The tumescent region is selected, and its volume and spatially averaged ADC are plotted in c).

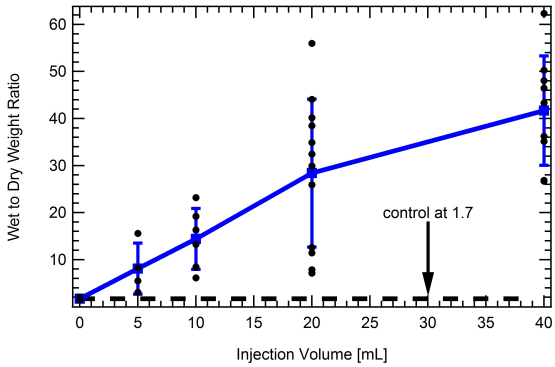

Figure 5: The degree of swelling of tumesced tissue is characterized by its wet-to-dry weight ratio. Comparing to the wet-to-dry weight ratio of control samples gives the degree of expansion. The scatter amongst injections of the same volume is due to spatial variations within the same tumescence.

otic will reach the pocket via diffusion.

DW-MRI is a non-invasive method of measuring the apparent diffusion constant (ADC) within tissue (Bihan et al., 1986). Various volumes of saline were infused successively into both right and left thighs of an anesthetized juvenile Yucatán pig, and DW-MRI images were taken to quantify the size of tumescence and the ADC as a function of total volume infused (0, 5, 10, 20, 40 mL). The image resolution was $1 \times 1 \times 5$ mm, and the ADC was acquired using 5 b values (0, 50, 100, 400, 800 s mm^{-2}).

Figure 4 a) is an axial image intersecting the tumescence (large light region) in the left leg after 40 mL was infused. Lineouts crossing the tumescence (figure 4 b)), have a zero ADC value in empty space, and about $1.4{\cdot}10^{-3}$ mm^2 s^{-1} in the muscle underneath the tumescence, consistent with the literature (Schwenzer et al., 2009). Amazingly, within the tumescence, the ADC saturates at a value equal to the self-diffusion coefficient of water, $2.5{\cdot}10^{-3}$ mm^2 s^{-1} (Wang, 1965), for even the smallest injection performed, 5 mL. Even for such small injections, the tissue has expanded enough where the structure of the interstitial matrix negligibly restricts diffusion. As more fluid is infused, the tumescence expands both into the empty space above the skin, but also into the body below. Not shown, is that in addition to the thickness growing, the area covered broadens as well. The total volume of the tumescence gives a measure of the average degree of expansion (figure 4 c)). For instance, when 20 mL were infused, the high-ADC volume was 30 mL, meaning that 10 mL of tissue expanded to 30 mL, and so the average degree of expansion was 3×. For 5, 10, and 40 mL, the degree of expansion was 2.25, 2.25, and 3.7× respectively.

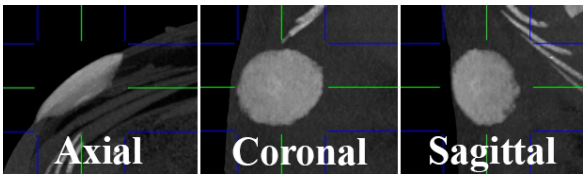

Figure 6: Three orthogonal CT views of a 20 mL tumescent injection into the abdomen of an adult Yucatán pig, viewed in maximum-intensity-pixel (MIP) mode. Green and blue lines indicate the center and extent of the MIP slabs.

However, there is considerable variation in the degree of expansion within each tumescence, as indicated by the visible white streaks within the blue region in Figure 1. To get a feel for the amount of variation, 5-11 small samples (about 0.5 g each) were cut off from the much larger tumescence, and weighed before and after desiccation. While taking samples, we attempted to avoid regions with visible white streaks (presumed to be fatty tissue) and focused instead on the more transparent, high-expansion regions. The fatty regions are expanded as well, but to a lesser degree. Consequently, the points on the graph should be interpreted as representative of local maxima in expansion, not random samples. For the smaller volume injections, it was difficult to avoid the streaks embedded within the tumescence and more found their way into the samples. The wet-to-dry-weight-ratio is shown in figure 5 for various volumes injected, and is roughly proportional to volume injected. Control samples, taken from regions without injection, have a wet-to-dry-weight-ratio of 1.7, while tissue tumesced with 20 mL saline had regions with ratios of 10-50, which implies an expansion of 6-30×.

The fluid doesn't remain in place very long; pressure gradients act to distribute it, and the resulting flow further assures the fluid is well-dispersed. We observe distinct processes as the tumescence returns to normal. Once the injection is complete, a pressure gradient exists between the tumesced site and the surrounding tissue, and the tumescence slowly expands and softens on the few minute timescale. This process is characterized by fluid flow within the subcutaneous tissue in the regions near the injection and is observed in live and dead pigs. In live pigs, we also observe the circulation absorbing the fluid and distributing it through the body on a multi-hour timescale. We have studied the rapid, local spreading with computed tomography (CT) as well as 3D-scanning.

Eight tumescent injections were made in the abdomen of an anesthetized adult Yucatán pig, 2 each of 2.5 mL, 5 mL, 10 mL, and 20 mL saline solution containing 20 mg mL^{-1} iodine contrast (6 mL Omnipaque 350 diluted to 100 mL). CT scans (resolution of $1 \times 1 \times 1$ mm) were made every 5-10 min for 70 min. Figure 6 displays three orthogonal views of one of the 20 mL injections immediately after the injection. The volume and mean attenuation within each tumescence were measured, and are displayed in figures 7 a) and b) respectively. For comparison, the attenuation of the pure solution (saline and contrast) and normal subcutaneous tissue were measured to be 500 HU and -90 HU respectively. Note that there is a rise in the tumescent volume during the first 5-10 min, corresponding with a drop in the mean attenuation. This reflects the fluid spreading within the subcutaneous tissue, overtaking more unexpanded tissue, but staying localized. Multiplying the mean attenuation by the volume gives the total contrast curve in figure 7 c). If the contrast was being taken away from the tumescence by the circulation, this curve would

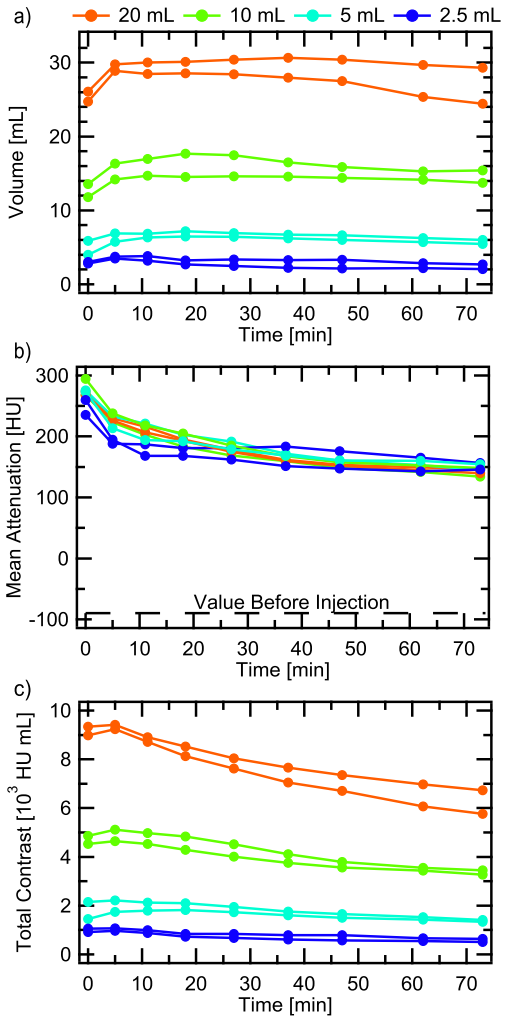

Figure 7: The evolution of different volume tumescent injections over an hour as measured by CT.

decrease, and so its initial flatness confirms our localized spreading interpretation. On longer timescales, we do see slow absorption by the circulation. Once again we can estimate the average expansion by comparing the mean attenuation within the tumescence (200-300 HU depending on the time after injection) to that before (-90 HU) and that in the pure solution (500 HU), yielding expansions of 3-5×, consistent with our previous estimates.

We studied the evolution of the tumescent skin profile with a Fuel-3D Scanify 3D camera. A 20 mL tumescent injection was performed in the abdomen of a dead juvenile Yucatán, and 3D photographs were taken periodically for 20 min. Figure 8a) shows the raw data before and immediately after injection. Note that the Z-scale is 10× smaller than the X and Y scale. Lineouts along Y and X are shown in figures 8b) and c) respectively for various times after the injection. It is clear that the tumescence changes shape very rapidly early on, dropping more in the first two minutes than in the subsequent seventeen. After about 10 min, changes are imperceptible, less than the uncertainties of our measurement. The contour maps of figures 8e) and f) show the difference between the skin profile at t=0 or t=19 min respectively and the profile before the injection. Plotting the max difference and cross-sectional area at half-max over time gives figure 8d). The product of the height and area curves, proportional to the tumescent volume, is constant within uncertainties. We fit the data with stretched exponential curves ($\mathrm{Exp}[-(t/\tau)^{\beta}]$, τ is in the range of 2-5 min, and $.5 < \beta < .8$), but we admittedly do not have any reason to expect such a form for the decay. There is an open theoretical question of the expected form of such a flow based on Darcy's law in a medium whose permeability depends on the degree of expansion (coupled flow and gel mechanics, see Netti et al. (2003)). Since the 3D-scan data was acquired on a dead pig, there is no circulation to distribute the injection through the body, and we are assured that the observed dynamics are purely flow in the interstitial matrix. In a live pig, when the local spreading slows enough, the circulation becomes the dominant mechanism of further distribution.

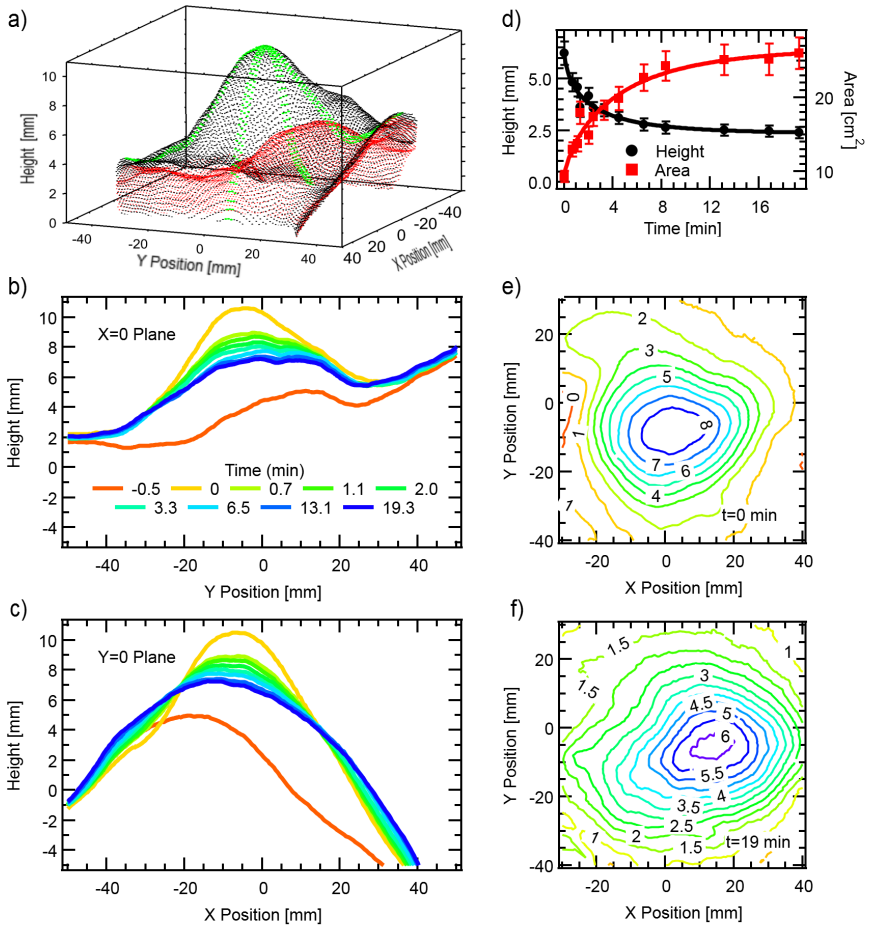

Figure 8: 3D scans yield the tumescent skin profile over time. Panels b) and c) are lineouts of the full 3D data, shown immediately before (red) and after (black) injection in panel a). Two perpendicular green lines are drawn along the tumescent surface in a) to help guide the eye. The difference between the skin surface at various times after the injection, with that before the injection, is used to calculated the tumescent height and cross-sectional area at half-height, d). Panels e) and f) are contour plots of the difference at times t=0 and t=19 min respectively.

Tumescent injections reside for hours

Eventually the tumescence dissipates and the interstitial tissue returns to normal, but the timescales of this process were not measured directly before this work. Indirect estimates based on plasma lidocaine concentrations following tumescent liposuction (Klein, 1993) suggest that the tumescence exists $\sim$ 10 hr. But tumescent fluid used for anesthesia usually contains dilute epinephrine, a vasoconstrictor, to minimize blood loss and slow down the rate of lidocaine absorption (Rubin et al., 1999). We expect epinephrine would also extend the tumescence residence time.

We performed CT scans periodically over seven hours to see the tumescence dissipate both with and without epinephrine. As before, eight tumescent injections were made in the abdomen of an anesthetized adult Yucatán pig, 2 each of 2.5 mL, 5 mL, 10 mL, and 20 mL saline solution containing 20 mg mL^{-1} iodine contrast (6 mL Omnipaque 350 diluted to 100 mL). A few weeks later, we performed the same experiment, with the addition of 1:100 000 epinephrine to the tumescent solution.

Coronal images in maximum-intensity-pixel (MIP) mode are shown in figures 9 and 10 without and with epinephrine respec-

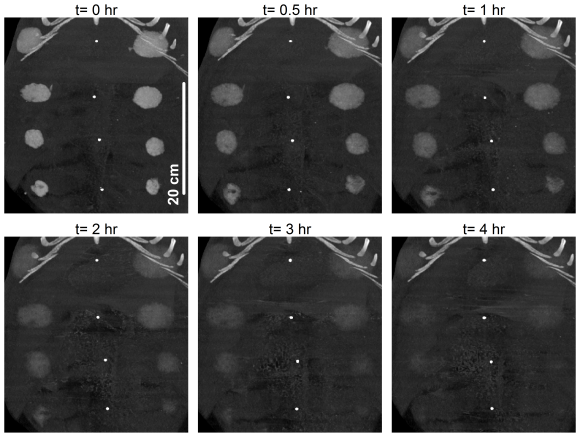

Figure 9: CT coronal images in MIP mode showing the time evolution of various volume tumescent injections of saline with iodine contrast into abdominal subcutaneous tissue of an adult Yucatán pig. Two injections of 20 mL, 10 mL, 5 mL, and 2.5 mL each were done on opposite sides of the pigs abdomen, with large volume injections closer to the pigs head (top of images) and smaller ones towards the feet (bottom of images). The white dots along the center of the abdomen are markers placed in the same axial plane as the injection location. Images for $t > 4$ hr are not shown because the injections are difficult to see.

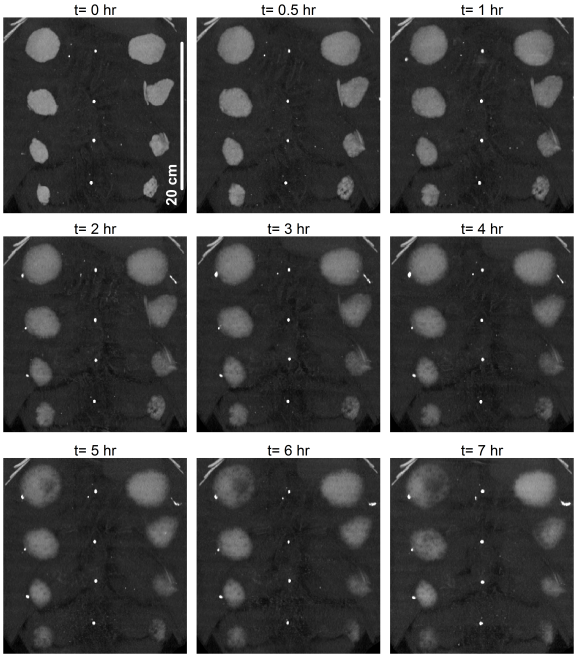

Figure 10: CT coronal images in MIP mode showing the time evolution of various volume tumescent injections of saline with iodine contrast and 1:100 000 epinephrine into abdominal subcutaneous tissue of an adult Yucatán pig. Volumes and location of tumescent injections are the same as in figure 9. The white dots along the center of the abdomen are markers placed in the same axial plane as the injection location. The white dots that form on the side of the tumescent spots in the later images are tumescent fluid leaking out of the puncture wounds.

tively (all images have the same contrast setting). In both cases, localized spreading occurs between the $t = 0$ and the $t = 0.5$ hr images, as indicated by the tumescence boundary becoming less sharp; we did not expect epinephrine to affect this. As time progresses, the tumescence fades away. Without epinephrine, it is hard to see any remaining contrast after three hours. With epinephrine, it is easily visible after seven hours. For a more precise comparison, we took lineouts crossing the center of each spot, seen in figure 11, and plotted the peak value vs time in figure 12. Attenuation levels after six hours in the presence of epinephrine are comparable to those after half an hour without epinephrine. However, even without epinephrine, the contrast remains substantially localized for 2-3 hr for the larger injections. In general, the larger injections decay somewhat slower.

On the question of time duration required for concentrated antibiotic to eradicate an infection, we offer some comments. Since bacteriostatic drugs work by preventing the growth of bacteria, we can estimate that that drug should remain concentrated for several bacteria doubling times. Doubling times during the exponential-growth phase are 20-40 min for most MRSA and other common strains (Okuma et al., 2002; Powell, 1958), and so a residence time of a few

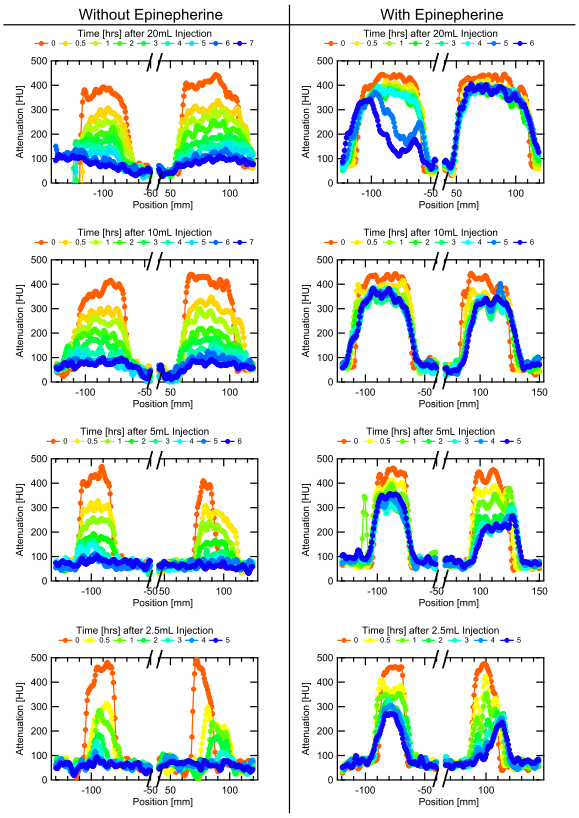

Figure 11: Lineouts crossing the center of the tumescent spots in figures 9 and 10.

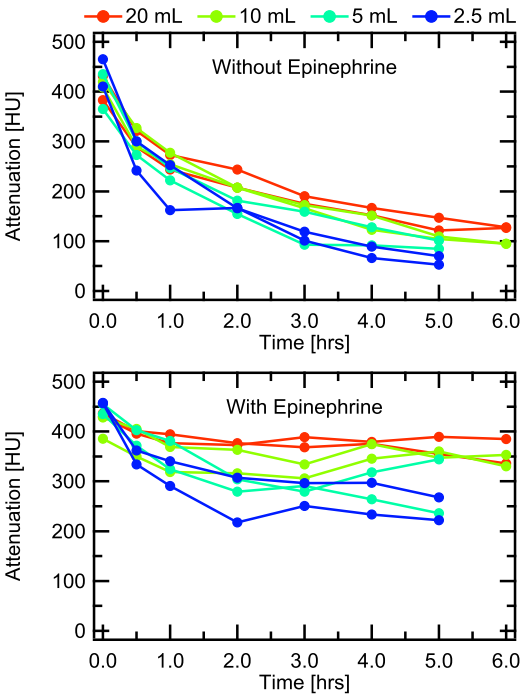

Figure 12: Decay of CT attenuation as the circulation removes tumescent fluid from the injection site. Epinephrine dramatically increases the tumescence residence time.

hours satisfies this requirement. Bacteria in chronic wounds, however, might not be in the exponential-growth phase, so longer times might be needed. On the other hand, bacteriostatic drugs often become bactericidal at high concentrations (Pankey and Sabath, 2004), whereupon the doubling-time-scale is no longer applicable. Further studies are needed to provide a definitive answer.

Conclusion

Tumescent injections force the expansion of subcutaneous tissue from the inside out, opening up pores, and saturating the interstitial matrix with fluid. The fluid residence time is 2-3 hr without any special preparation, and can be extended several times with the use of epinephrine. The criteria we raised in the introduction, by which we judge if tumescent antibiotic injections have a chance of being effective, have been met. Could this be an effective method of treating antibiotic-resistant infections? Interestingly, there *is* a procedure currently in FDA phase 2 clinical trials (Sonescence, Inc., 2010) that uses tumescent antibiotic injections (10 mg mL^{-1} Cefazolin), but with a twist. After the injection, therapeutic ultrasound is applied to the skin surface, and claimed to disperse the antibiotic within the tissue. The injection and ultrasound combination has successfully treated 108 patients off-label or under an institutional-review-board-approved

phase 1 pilot study (Sonescence, Inc., 2014), including many with drug-resistant infections. Tumescent injections without external ultrasound have not been tried. It may be that the ultrasound is essential, but given the physical picture we present, we wonder if the injection would work equally well on its own.

The use of all animals in this study was approved by the UCLA Animal Research Committee.

Acknowledgments

We gratefully acknowledge support from the Paul S. Veneklasen Research Foundation. We thank Novena Rangwala and Barry Silberg for helpful discussions and Adam Collins, Seth Pree, Alexandra Latshaw, Genia Dubrovsky, Elvin Chiang, Adora Samaan and the UCLA DLAM staff for assistance.

References

Azevedo EF, Barbosa LA, Cassiani SHDB. Administration of antibiotics subcutaneously: an integrative literature review. Acta Paulista de Enfermagem, 2012;25:817 – 822.

Bihan DL, Breton E, Lallemand D, Grenier P, Cabanis E, Laval-Jeantet M. Mr imaging of intravoxel incoherent motions: Application to diffusion and perfusion in neurologic disorders. Radiology, 1986;161:401–407.

Duran-Reynals F. The effects of extracts of certain organs from normal and immunized animals on the infecting power of vaccine virus. J. Exp. Med, 1929;20:327–40.

Duran-Reynals F. Tissue permeability and the spreading factors in infection. Bacteriology Reviews, 1942;6:197–252.

Frasca D, Marchand S, Petitpas F, Dahyot-Fizelier C, Couet W, Mimoz O. Pharmacokinetics of ertapenem following intravenous and subcutaneous infusions in patients. Antimicrobial Agents and Chemotherapy, 2010;54:924–926.

Guyton AC, Scheel K, Murphree D. Interstitial fluid pressure: III. its effect on resistance to tissue fluid mobility. Cancer Research, 1966;19:412–419.

Hanke W, Cox SE, Kuznets N, III WPC. Tumescent liposuction report performance measurement initiative: National survey results. Dermatologic Surgery, 2004;30:967–977.

Harb G, Lebel F, Battikha J, Thackara JW. Safety and pharmacokinetics of subcutaneous ceftriaxone administered with or without recombinant human hyaluronidase (rHuPH20) versus intravenous ceftriaxone administration in adult volunteers. Current Medical Research and Opinion, 2009;26:279–288.

Klein J. Tumescent technique for regional anesthesia permits lidocaine doses of 35 mg/kg for liposuction. The Journal of dermatologic surgery and oncology, 1990;16:248–263.

Klein JA. The tumescent technique for lipo-suction surgery. The American Journal of Cosmetic Surgery, 1987;4:263–267.

Klein JA. Tumescent technique for local anesthesia improves safety in large-volume liposuction. Plastic and Reconstructive Surgery, 1993;92:1085–1098.

Netti PA, Travascio F, Jain RK. Coupled macromolecular transport and gel mechanics: Poroviscoelastic approach. Bioengineering, Food, and Natural Products, 2003;49:1580–1596.

Nicolau DP, Silberg BN. Assessing the potency of cefazolin against methicillin-resistant staphylococcus aureaus (MRSA): Microbiologic data supporting ultrasonic drug dispersion for the management of skin & skin structure infections (SSSIs). 55th Interscience Conference on Antimicrobial Agents and Chemotherapy/International Congress of Chemotherapy and Infection, San Diego, 2015.

Okuma K, Iwakawa K, Turnidge JD, Grubb WB, Bell JM, O'Brien FG, Coombs GW, Pearman JW, Tenover FC, Kapi M, Tiensasitorn C, Ito T, Hiramatsu K. Dissemination of new methicillin-resistant *Staphylococcus aureus* clones in the community. Journal of Clinical Microbiology, 2002;40:4289–4294.

Pankey GA, Sabath LD. Clinical relevance of bacteriostatic versus bactericidal mechanisms of action in the treatment of gram-positive bac-

terial infections. Clinical Infections Diseases, 2004;38:864–870.

Powell EO. An outline of the pattern of bacterial generation times. J. gen. Microbiol., 1958;18:382–417.

Rubin JP, Bierman C, Rosow CE, Arthur GR, Chang Y, Courtiss EH, Jr. JWM. The tumescent technique: The effect of high tissue pressure and dilute epinephrine on absorption of lidocaine. Plastic and Reconstructive Surgery, 1999;103:990–996.

Schwenzer N, Steidle G, Martirosian P, Schraml C, Springer F, Claussen C, Schick F. Diffusion tensor imaging of the human calf muscle: distinct changes in fractional anisotropy and mean diffusion due to passive muscle shortening and stretching. NMR Biomed., 2009;22:1047–1053.

Sonescence, Inc. Direct antibiotic delivery of cefazolin into soft tissue infections using subcutaneous injection and ultrasonic dispersion (DAD), 2010. ClinicalTrials.gov [Internet]. Bethesda (MD): National Library of Medicine (US). 2000-[cited 2017 Feb 01]. Available from: https://clinicaltrials.gov/ct2/show/NCT01238276 NLM Identifier: NCT01238276.

Sonescence, Inc. Our history, 2014. URL `http://www.sonescence.com/our-history`

Swabb EA, Wei J, Gullino PM. Diffusion and convection in normal and neoplastic tissues. Cancer Research, 1974;34:2814–2822.

Wang JH. Self-diffusion coefficients of water. J. Phys. Chem., 1965;69:4412–4412.